Annals of Parasitology 2022, 68(1), 23–34
doi: 10.17420/ap6801.404

Original paper

Evaluation of deltamethrin-loaded Zn-Fe, Zn-Al-GA layered double hydroxide, and Fe-O nanoparticles against resistant *Rhipicephalus annulatus* ticks

Shawky M. ABOELHADID[1], Samar M. IBRAHIUM[2], Ahmed A. WAHBA[3], Ahmed A. FARGHALI[4]

[1]Department of Parasitology, Faculty of Veterinary Medicine, Beni-Suef University, Beni-Suef, Egypt
[2]Department of Parasitology, Animal Health Research Institute, Fayum Branch, Fayum, Egypt
[3]Department of Parasitology, Animal Health Research Institute, Dokki, Egypt
[4]Materials Science and Nanotechnology Department, Faculty of Postgraduate Studies for Advanced Sciences, Beni-Suef University, Beni-Suef, Egypt

Corresponding Author: Shawky M. Aboelhadid; e-mail: shawky.abohadid@vet.bsu.edu.eg

ABSTRACT. The over use of deltamethrin has resulted in the development of resistance. Thus, the search for a new method to improve its acaricidal effect is the target of the present study. Layered double hydroxide (LDH) compounds are now used as drug delivery systems. Deltamethrin (Butox®) was loaded on Zn-Fe LDH, Zn-Al-GA layered double hydroxide (LDH), and Fe-oxide nanoparticles NPs. Then its acaricidal efficacy was evaluated. The nanocomposites (NCs) were prepared by the co-precipitation method and characterized before and after deltamethrin loading. The deltamethrin-loaded NCs were applied against the phenotypically resistant *Rhipicephalus annulatus* tick (adult and larvae). The adult ticks treated by Butox® alone or Butox® loaded nanocomposites at different concentrations showed no mortality. A significant ($P \leq 0.05$) reduction in egg production index was observed at the recommended dose (X) (1 µl/ml distilled water) and its bi-folds (2X, 3X, and 4X) in ticks treated with deltamethrin/Zn-Fe LDH nanocomposites compared to deltamethrin alone. Moreover, no significant difference ($P > 0.05$) was recorded in larval mortality between the treatments with deltamethrin alone and its loaded nanocomposites. Also, the nanomaterials alone without conjugation with deltamethrin revealed a low mortality rate. Deltamethrin-loaded nanocomposites even improve effect against adult tick but cannot overcome tick resistance to deltamethrin that needs more search. The acaricidal activity of deltamethrin was not improved after loading it with these nanocomposites.

Keywords: deltamethrin, *Rhipicephalus annulatus*, resistance, layered double hydroxides, Zn-Fe LDH, Zn-Al-GA LDH, Fe-O NPs

Introduction

Rhipicephalus annulatus is an important ixodid tick, widely spread in tropical areas [1]. This tick causes significant economic loss due to its effect on cattle production [2] and is considered a vector for fatal infectious diseases including babesiosis, and anaplasmosis [3,4]. In Egypt, *R. annulatus* is the common tick species infesting cattle [5]. The common method used for tick control is the use of synthetic chemical acaricides [6]. The resistance of *R. microplus* to pyrethroids and organophosphates was recorded globally [7]. Also, pyrethroid-resistant populations of *R. annulatus* in Egypt were reported [5,8]. Moreover, synthetic chemical acaricides, including deltamethrin, have been widely used to control animal ectoparasites and insect pests (mosquitoes, cockroaches, flies, and fleas) in households [9].

Layered double hydroxid (LDHs) (hydrotalcite-like) compounds have special characters like particle size, easy control, good biocompatibility, and high loading capacities [10]. The LDH layer-drug intercalation was applied in drug delivery and in water decontamination [11–14]. The LDH nanomaterials have several uses in cancer therapy,

cosmetics, and removal of toxic metals from contaminated water [15–18]. The Zn-Al LDH and Mg-Al LDH were used in bone healing [19]. The doxycycline/LDH and amoxicillin/LDH prevented ulcer formation and improved wound healing on experimental animals (rats) [20]. Iron nanoparticles are characterized by easy synthesis, low toxicity, high diversity and antimicrobial effect. Accordingly, it is used in drug delivery systems, and imaging for the diagnosis of diseases [21], in anemia, and in cancer treatments [22].

Therefore, it is necessary to investigate synthesized nanoparticles, which are less likely to cause ecological pollution and improve the efficacy of the acaricides [23,24]. Synthesized metal nanoparticles, such as silver nanoparticles, zinc oxide nanoparticles, silicon oxide nanoparticles, and titanium dioxide nanoparticles have been used with some essential oils and herbal extract to control ticks [23–26]. Moreover, Aboelhadid et al. [27] used *Ocimum basilicum* essential oil loaded LDH to improve its acaricidal efficacy against resistant *R. annulatus*, and recorded a significant effect larvicidal and repellency effect on larvae. To increase the acid-resistant properties of LDH composites, the surfaces can be covered with unsaturated fatty acids such as oleic acid. Because of their high stability in acid solution, these composites are used in drug delivery to the intestine, as they are unaffected by the stomach's strongly acidic gastric juices [28].

Consequently, the efficacy of Zn-Fe LDH-NPs, Zn-Al-GA LDH-NPs, and Fe-NPs alone or combined with deltamethrin were investigated against larvae and adults of *R. annulatus*.

Materials and Methods

Commercial deltamethrin 5% (Butox®, EC; 5% active ingredient, Arab Company for Chemical Ind. Cairo, Egypt) was used for synthesis of Zn-Fe LDH, Fe-NPs, Zn-Al-GA LDH nanoparticle-functionalized deltamethrin hybrids. The nanomaterials were provided by Professor Ahmed A. Farghali (Materials Science and Nanotechnology Department, Faculty of Postgraduate Studies for Advanced Sciences, PSAS, Beni-Suef, University, Beni-Suef, Egypt). Deltamethrin, deltamethrin/Zn-Fe LDH, deltamethrin /Fe-NPs and deltamethrin/Zn-Al-GA LDH composites were evaluated against adult ticks and larvae at different concentrations (recommended dose (X) = 1 µl/ml distilled water, 2X, 3X, and 4X).

Preparation of nanoparticles
Zn-Fe LDH, Zn-Al-GA LDH and Fe-oxide nanoparticles

The co-precipitation method was used for preparations of Zn-Fe LDH (4:1) and Zn-Al-GA LDH (4:1:1) nanocomposites [29]. Zinc and iron nitrates were mixed together at a 4:1 molar ratio in 50 ml distilled water at room temperature. During continuous stirring, sodium hydroxide (2 mol/l) was added drop by drop to pH 8.0 with stirring for 24 h until precipitation of Zn-Fe LDH completed. The same mixing of zinc and aluminum chlorides, and GA at molar ratio (4:1:1) for Zn-Al LDH/GA preparation. The resulted precipitate was filtered and washed several times with distilled water at pH 7.0. The filtrate was kept in a vacuum oven dryer at 50°C for 24 h. The Fe-O NPs were prepared by employing the bud extract of clove (*Syzygium aromaticum*). Five grams from dried grinding clove buds were washed with distilled water twice to remove dust, then mixed with 250 ml distilled water, and heated for 10 min. at 100°C. After cooling in room temperature, the resultant extract was centrifuged and filtered with No. 1 Whatman filter paper. The filtrate was used for Fe-NP synthesis. Fifteen ml clove extract were mixed with 5 ml of 0.3 molar iron nitrate (adjusted with 0.1 molar NaOH to pH~6) and incubated at room temperature for 10 hours. The synthesized Fe NPs were centrifuged, washed three times with distilled water followed by ethanol, dried at 40°C, and kept for characterization. Green synthesized Fe NPs were calcined for 4 h at 550°C in oven under air.

Loading of deltamethrin on nanomaterials

Deltamethrin/Zn-Fe LDH, deltamethrin/Zn-Al-GA LDH, and deltamethrin/Fe-NPs were prepared by repeating the same procedures using different concentrations of deltamethrin in each nano-suspension. Subsequently, the deltamethrin/NP suspensions were stirred at room temperature for 20 h, filtrated through No. 1 Whatman filter paper, washed by distilled water, and dried at 40°C, respectively [20].

Characterization of nanomaterials

FeO-NPs, Zn-Fe LDH, and Zn-Al-GA LDH were characterized by X-ray diffraction on a PANalytical (Empyrean) X-ray diffraction with Cu-Kα radiation (wave length 0.154 nm). Fourier transform infrared spectroscopy (FTIR) was recorded on PerkinElmer FTIR Spectrum BX

(PerkinElmer Life and Analytical Sciences, CT, USA). The morphological characters of nano-particles were determined by images of field emission high resolution scanning electron microscope (Gemini, Zeiss-Ultra 55).

Efficacy of the synthesized/loaded deltamethrin nanocomposites against R. annulatus

Tick collection and hatching of larvae

Adult female ticks of *R. annulatus* ticks were collected from naturally infested cattle visiting veterinary clinics and farms in Fayum governorate from June through August 2020 (hot seasons). Ticks were collected in carton boxes containing a ventilation opening and transported to the Laboratory of Parasitology, Faculty of Veterinary Medicine, Beni-Suef University, Egypt. Tick samples were washed with distilled water to remove any debris and allowed to dry on filter paper. They were identified as *R. annulatus* under a stereo-binocular microscope with anterior and short mouthparts, small eyes or absent, no festoons and medium in size. The ticks were weighed, and divided into groups, 10 ticks in each group. Adults were kept in Petri dishes and used for the experiments. A part of adult female ticks was kept in a Bio-oxygen Demand (BOD) incubator at 37°C and 80% relative humidity until they laid a large number of eggs, then incubated for 14–18 days for hatching to obtain the larvae needed for larval bioassays.

Adult immersion test

The previously prepared solutions of deltamethrin, deltamethrin/Zn-Fe LDH, deltamethrin /Zn-Al-GA LDH, and deltamethrin/Fe NPs were tested against engorged female ticks of similar size. The engorged female ticks were immersed in 10 ml of the solution for 2 min., then dried, and incubated in BOD for 21 days in Petri dishes [30]. The treatments were divided into 10 ticks per group and five replications of each treatment were maintained. The control group was treated by immersion in 10 ml distilled water (DW) for 2 min. The mortality was observed daily in treated ticks. Eggs were collected from each group separately and weighed to calculate the egg production index EPI = (weight of eggs/initial weight of engorged tick)×100.

Larval packet test

Larvae of 14 days-old were used for bioassay. The filter paper was put in a Petri dish, and one ml of prepared nanocomposite solution was inoculated to the filter paper. The impregnated paper was allowed to dry and then folded to form packets. Larvae (approximately 100) were transferred with a brush into the experimental packet, which was sealed by bulldog clips. The treated packets were kept in a controlled environmental chamber set at 26–28°C and 80% relative humidity for 24 h. In the control group, nanomaterial solutions were replaced with distilled water [31].

Statistical analysis

Data of tick biological parameters were analyzed statistically using the Statistical Package for Social Science (SPSS for Windows (IBM), version 22, Chicago, USA) to determine if variables differed between nanomaterials. In addition, ANOVA tests were applied to determine the differences between means. The results are denoted by the symbol ± SE. Probability values of less than 0.05 (P<0.05) were considered significant.

Results

Characterization of NCs and its loading with deltamethrin

Deltamethrin loaded with Zn-Fe/LDH, Zn-Al-GA/LDH and Fe-NPs was confirmed by XRD, SEM, and FT-IR. The prepared Zn-Fe LDH was similar to typical XRD patterns of hydrotalcite-like LDH materials. The Zn-Fe LDH was highly crystalline with sharp diffraction peaks. The layered structure of Zn-Fe LDH was confirmed by the presence of main peaks at 2θ at 31.86°, 34.6°, 36.4°, and 47.62° corresponding to (003) plane. The comparison between XRD before and after deltamethrin loading revealed that the decrease of some diffraction peak intensity, e.g., 34.55°, 36.47°, 47.41°, 68.04°. The diffraction angle was at 23.7° and 59.7° in the pattern of XRD after conjugation and belongs to the deltamethrin. The basal peak (2θ°=36.4755°) in the deltamethrin/Zn-Fe LDH concise to an interlayer-layer distance of 2.46337 A°, which was slightly higher than that in Zn-Fe LDH by 0.00047 A°. This means that the deltamethrin was not intercalated in the Zn-Fe LDH layers but the high-intensity peaks of 2θ values (36.4827° and 36.4755°) for Zn-Fe LDH and deltamethrin/Zn-Fe LDH, respectively, were due to the interaction of deltamethrin with metal cations, Zn(II) and Fe(III) of the LDH (Fig. 1) The prepared Zn-Al-GA/LDH look liked the typical XRD patterns of hydrotalcite-

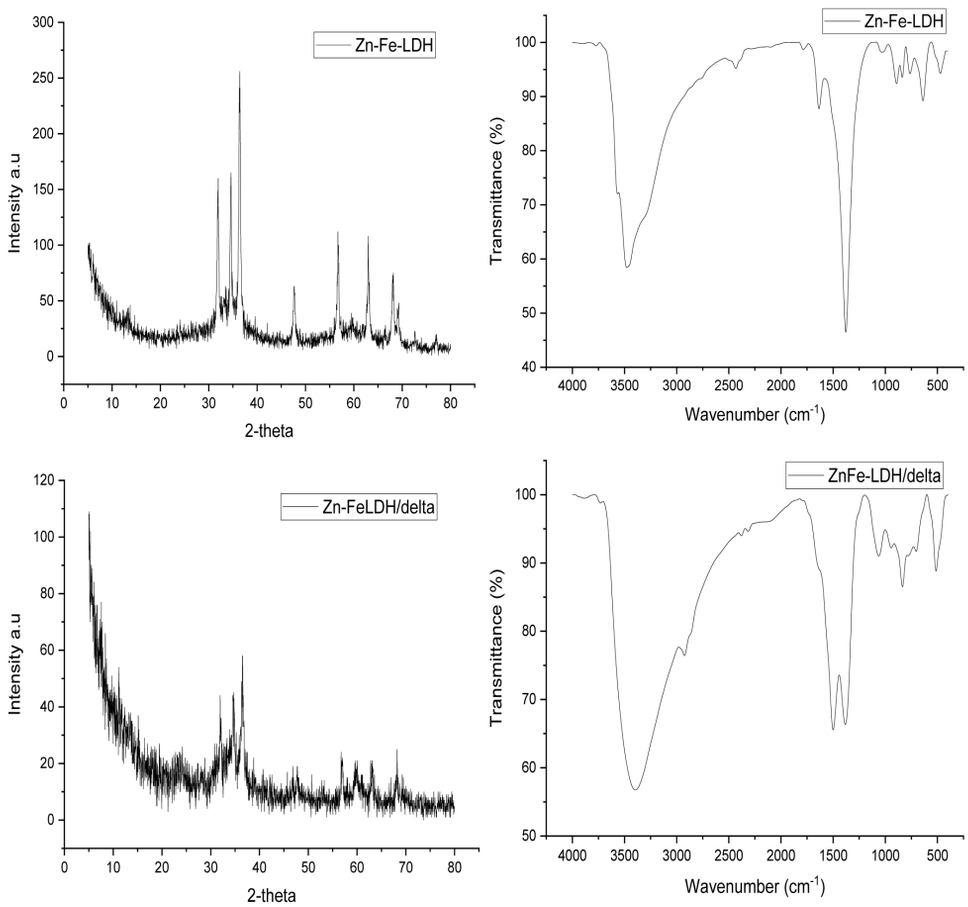

Figure 1. Zn-Fe LDH before and after conjugation with deltamethrin by XRD and FT-IR

like LDH materials with 33.50 nm crystallite size. In the XRD pattern before and after conjugation with deltamethrin, some diffraction peaks intensity were decreased, e.g., 27.87°, 34.54°, and 40.32°. The diffraction angle at 54.07° in the pattern of XRD after loading belonged to the deltamethrin. This decrease in the intensity of some peaks confirmed the occurrence of some diffusion process in the hexagonal structure of the synthesized parent LDH. In the XRD pattern of Zn-Al-GA/LDH/ deltamethrin, some peaks became broad e.g., 9.87°, 13.03°, and 19.92°, which is due to the presence of deltamethrin that caused exfoliation to layers of LDH and the exfoliated layers became stacked. Therefore, the sequential structure of LDH was hidden (Fig. 2). After calcination of green clove Fe-oxide, the crystallinity of magnetite or hematite green clove synthetized Fe-oxide became clear, due to the removal of most organic components by heat, and most of the prepared sample converted to magnetite while the rest turned to hematite. The diffraction peaks of calcinated green clove Fe-oxide were matched with that of the hematite and magnetite XRD pattern in card number (04-015-9569 and 04-009-8420, respectively). The mean diffraction peaks of XRD pattern of deltamethrin/ Fe-oxide at 2θ at 33.2°, 35.69°, 49.58°, 54.13°, 64.08°, which matched well with the hematite XRD pattern (04-015-9569) with some peaks of low intensity, e.g., 35.6°, 57.66°, and 62.59°. This matched with magnetite XRD pattern (04-009-8420). The conversion of magnetite form of Fe-oxide to hematite form of Fe-oxide was observed due to interaction of deltamethrin with Fe-oxide. Therefore, the increased intensity of some peaks was detected, (e.g., 33.2°, 49.58°, and 54.13°) but others with decreased intensity, (e.g., 35.69°, 62.59°). This conversion from magnetite to hematite form was due to the magnetite form was less stable so agglomeration occurred by magnetostatic interaction and adsorption of oxygen (Fig. 3).

The conjugation between deltamethrin and nanomaterials (Zn-Fe LDH, Zn-Al-GA LDH and Fe-oxide) was confirmed by detection of the chemical interaction, the alternation in the chemical bonds, functional groups, and the shifts in the wave number of the peaks. The broadband located at

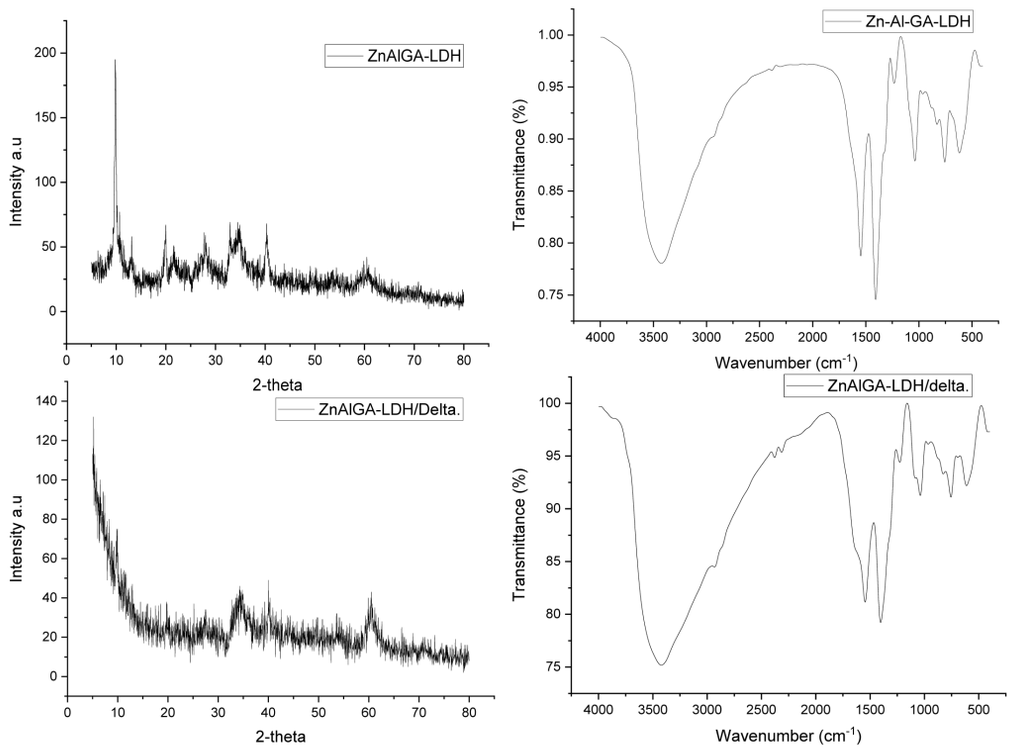

Figure 2. Zn-Al-GA LDH before and after conjugation with deltamethrin by XRD and FT-IR

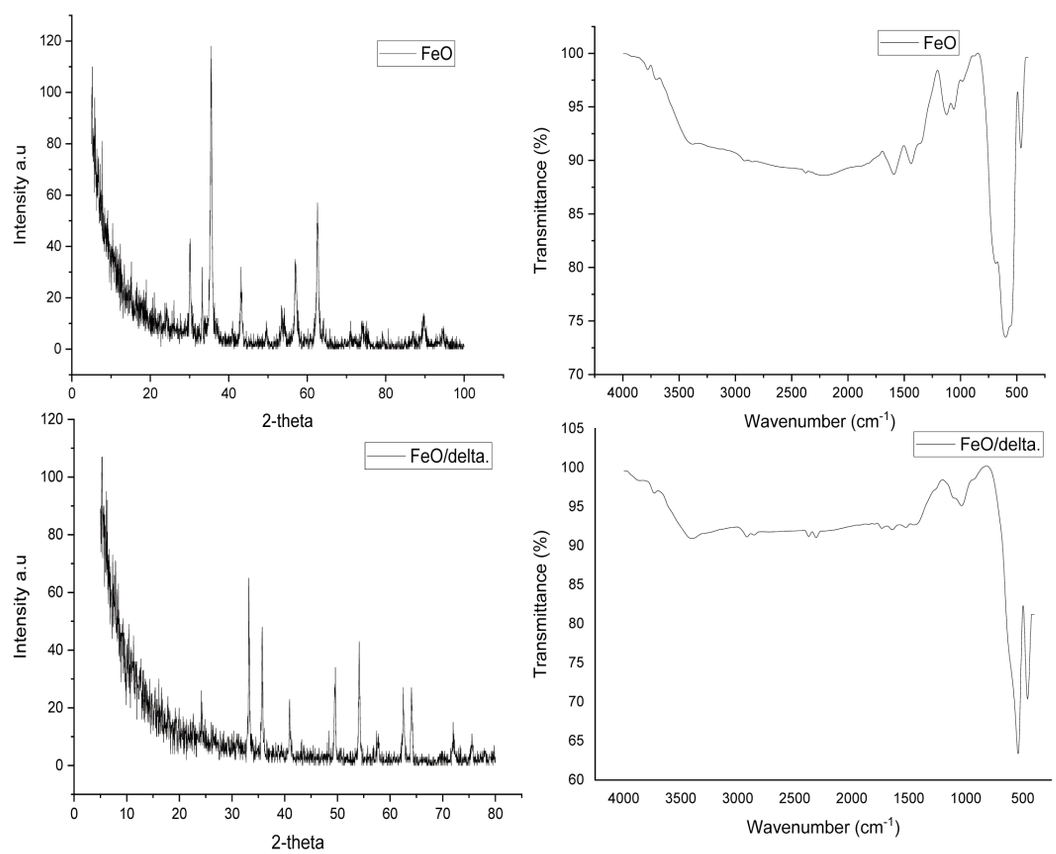

Figure 3. Fe-NPs before and after conjugation with deltamethrin by XRD and FT-IR

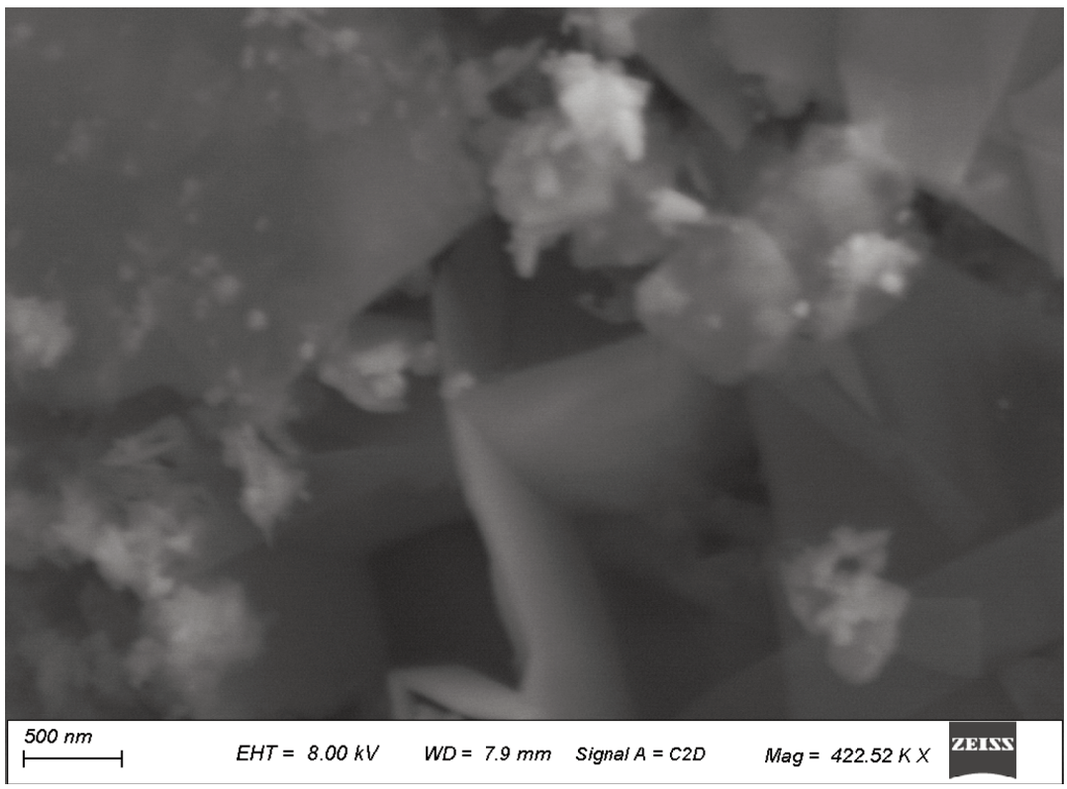

Figure 4. Scanning electron microscopy image of Zn-Fe/LDH

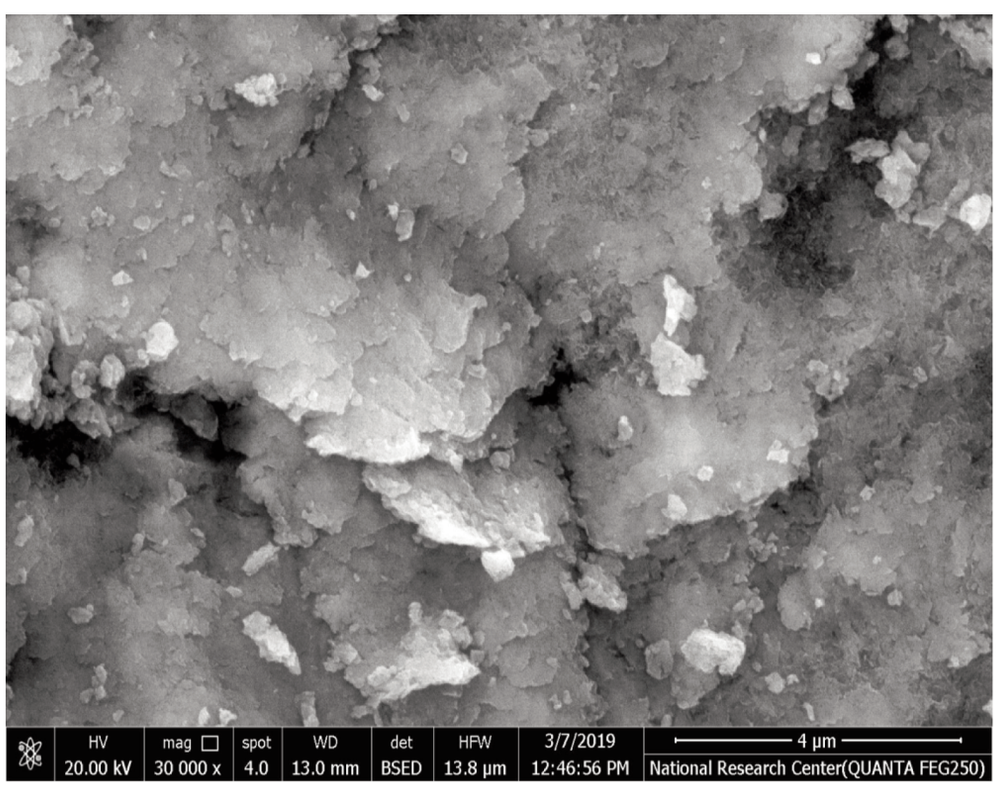

Figure 5. Scanning electron microscopy image of Zn-Al-GA LDH

3477.72 cm^{-1} resulted from the hydroxyl groups of layers stretching vibration and the interlayer water molecules. While the band at 1635.15 cm^{-1} produced from the bending vibration of water.

The characteristic peaks of loaded deltamethrin appeared at 1499.77 cm^{-1} for stretching vibration of

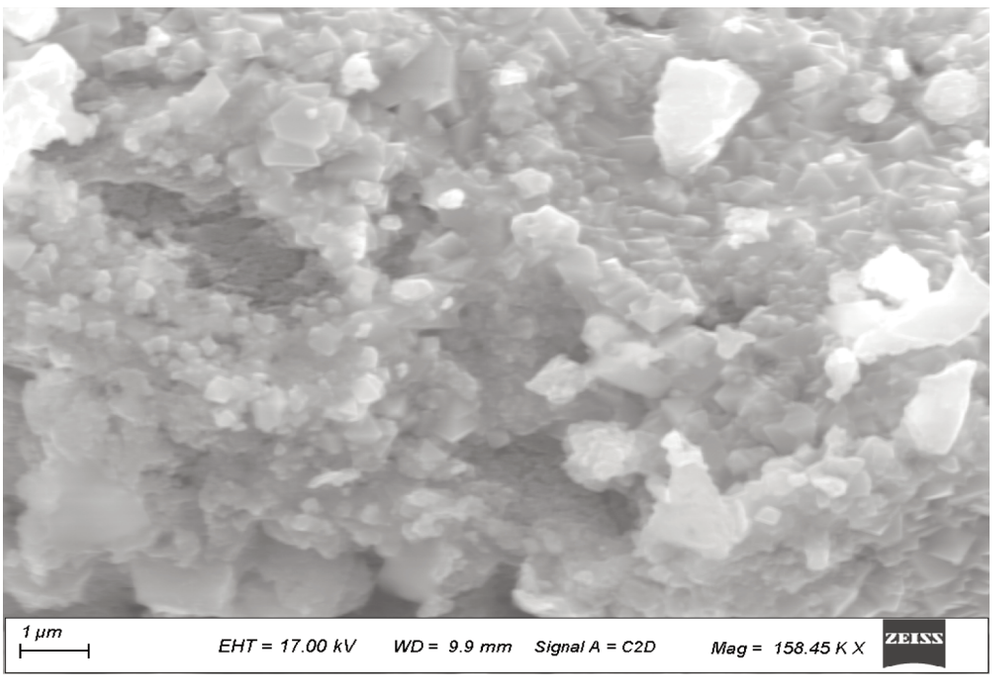

Figure 6. Scanning electron microscopy image of FeO

C=C groups, at 3396.04 cm^{-1} assigned to stretching vibration of the hydroxyl group, at 834.89, 943.05 and 2920.81 cm^{-1} resulted from the bending vibration of the C-H, at 1062.11 cm^{-1} was due to stretching vibration of a C-C bond. A weak peak appeared at 3731 cm^{-1} due to the stretching vibration of the N-H bond. Zn-Fe LDH had hydrogen donors (OH groups) on its surface, and there were hydrogen acceptors (-OH or -NH) in the structure of deltamethrin that supported the H-bonding formations. The OH vibration mode peak shifted from 3477 to 3396 cm^{-1} confirmed the deltamethrin interaction with Zn-Fe LDH (Fig. 1 and 2).

Spectra of Zn-Al-GA/LDH showed bands at 1546.98 cm^{-1} corresponding to C=C, at 1232.31 cm^{-1} assigned to COO- and at 1036.59 cm^{-1} resulting from phenol groups. The characteristic peak of loaded deltamethrin on Zn-Al-GA LDH showed at 2931.79 cm^{-1} corresponding to aliphatic CH2 and CH and at 692 cm^{-1} defined to the in-plane bending vibration of replacement benzene, referring to the presence of C=C. The increasing intensity and shifting of peaks referred to the formation of hydrogen bonds between H bond donor oxygen atoms and LDH layers, which confirmed conjugation of deltamethrin with Zn-Al-GA LDH (Fig. 2).

The FTIR spectra of Fe oxide before and after deltamethrin adsorption showed the absorbance bands of magnetite Fe-oxide appeared at 686 and 598 cm^{-1} and at 462 cm^{-1} for hematite Fe-oxide. The appearance of some peak vibration mode at 1643 and 1734 cm^{-1} and decreased the intensity of vibration peak at 457 and 540 cm^{-1} indicated interaction of deltamethrin with Fe-oxide and conversation of magnetite to hematite Fe-oxide due to disappearance of peak at 686 cm^{-1}(Fig. 3). The morphology of the synthesized materials was studied using FE-SEM. The FE-SEM images of both Zn-Al LDH/GA and Zn-Fe LDH represent a well-defined sheet structure as could be seen in figures 4 and 5. It is loose sheets in case of Zn-Fe LDH. However, the layers are compacted in case of the Zn-Al LDH/GA. The synthesized Fe-oxide NPs were characterized and clearly showed the formation of different spherical and compact small layer nanoparticles with various other shaped structures (Fig. 6).

Acaricidal bioassay of loaded deltamethrin nanocomposites

Adulticidal effect

No mortality in adult ticks occurred with deltamethrin alone or with deltamethrin-loaded nanocomposites at different concentrations. Only a significant reduction ($P \leq 0.05$) in egg production was observed at the recommended dose (X) and the folds of 2X, 3X, and 4X of ticks exposed to deltamethrin/Zn-Fe LDH nanocomposite when compared with that of deltamethrin alone, deltamethrin/Fe-NPs and deltamethrin/Zn-Al-GA

Table 1. Effect of deltamethrin and its freshly loaded nanocomposites against the resistant *Rhipicephalus annulatus* adult tick

Drug concentration		EPI % of deltamethrin	EPI % of deltamethrin /Zn-Fe LDH	EPI % of deltamethrin /Fe-NPs	EPI % of deltamethrin /Zn-Al-GA LDH
4X		18.81 ± 6.000	0.8806 ± 0.104*	34.94 ± 3.677	27.78 ± 12.48
3X		38.89 ± 12.60	8.806 ± 3.124*	48.95 ± 6.205	55.87 ± 5.449
2X		63.76 ± 9.773	22.78 ± 4.682*	61.84 ± 9.931	60.10 ± 11.66
X		66.55 ± 7.996	36.30 ± 12.39*	67.51 ± 2.890	69.98 ± 5.065
1/2X		74.77 ± 25.04	60.44 ± 14.88	74.20 ± 12.53	86.10 ± 10.96
1/4X		83.66 ± 8.889	65.23 ± 3.085	81.28 ± 4.342	87.29 ± 12.70
1/8X		86.90 ± 12.20	71.49 ± 7.426	89.91 ± 10.33	85.28 ± 11.94
Controls	Nanocomposites	76.32 ± 17.47	81.18 ± 8.660	81.92 ± 18.67	82.92 ± 9.976
	Control	91.96 ± 7.014	91.96 ± 7.014	91.96 ± 7.014	91.96 ± 7.014

Explanations: * – significant $P \leq 0.05$; EPI – egg production index; nanomaterials – Zn-Fe/LDH or Zn-Al-GA/LDH or Fe-NPs; X means recommended dose of deltamethrin (Butox®) (one µl/ml); EPI % of deltamethrin (egg production index percentage of ticks treated by deltamethrin); EPI % of deltamethrin/Zn-Fe LDH (egg production index percentage of ticks treated by deltamethrin conjugated with Zn-Fe LDH); EPI % of deltamethrin/Fe-NPs (egg production index percentage of ticks treated by deltamethrin conjugated with Fe-NPs); EPI % of deltamethrin/Zn-Al-GA LDH (egg production index percentage of ticks treated by deltamethrin conjugated with Zn-Al-GA LDH)

LDH nanocomposites. Deltamethrin and its loaded forms did not cause mortality or reduction in egg production at low concentrations of 1/8X, 1/4X, and 1/2X. A significant decrease in the egg production index (EPI) was reported at X, 2X, 3X, and 4X doses of Zn-Fe LDH/deltamethrin (36.3, 22.78, 8.80 and 0.88%) in comparison with the EPI of deltamethrin alone (66.5, 63.7, 38.8 and 18.8%), deltamethrin/Fe-NPs (67.5, 61.8, 48.9 and 34.9%), deltamethrin/Zn-Al-GA LDH NPs (69.9, 60.1, 55.8 and 27.7%), and the control (DW) group (91.9%) (Tab. 1).

Larval mortality

There was no significant difference in the larval mortality percentage of deltamethrin alone and deltamethrin-loaded Zn-Fe LDH, Fe-NPs, and Zn-Al-GA LDH nanoparticles. The larval mortality was 78.9, 85.3, 100 and 100% for deltamethrin alone, and 79.0, 85.9, 100 and 100% for deltamethrin/Zn-Fe LDH, and 83.6, 88.9, 100 and 100% for deltamethrin/Zn-Al-GA LDH, and 84.7, 93.8, 100 and 100% for deltamethrin/Fe-NPs at different concentrations of X, 2X, 3X and 4X, respectively (Fig. 7). The calculated LC50 was (0.77X, 0.78X, 0.73X and 0.70X for deltamethrin, deltamethrin/Zn-Fe LDH, deltamethrin/Zn-Al-GA LDH and deltamethrin/Fe-NPs, respectively (Tab. 2). Moreover, the LC90 was 1.74X, 1.72X, 1.57X, and 1.37X, for the same materials respectively (Tab. 2). No significant difference ($P \geq 0.05$) in mortality was observed when the different concentrations (4X, 3X, 2X, and X) were used for treatment against larvae. Whereas, the larval mortality was 100% at 4X and 3X of deltamethrin-loaded nanocomposites and deltamethrin alone. Additionally, no significant difference was observed in the larval mortality (ranging from 85.3–93.8 %) against X and 2X concentrations of deltamethrin loaded nanocomposites and deltamethrin alone were recorded. Larval mortality gradually decreased at low concentrations of deltamethrin and deltamethrin-loaded nanocomposites (1/2X, 1/4X, and 1/8X). Also, the nanomaterials alone (Zn-Fe LDH, Zn-Al-GA LDH, and Fe-NPs) without conjugation with

Table 2. LC50 and LC90 of deltamethrin and its freshly loaded nanocomposites *Rhipicephalus annulatus* larvae

Drug	LC50	LC90
Deltamethrin	0.775 X	1.741 X
Deltamethrin/Zn-Fe LDH	0.776 X	1.727 X
Deltamethrin/Zn-Al-GA LDH	0.732 X	1.574 X
Deltamethrin/Fe-NPs	0.702 X	1.37 X

X means recommended dose of deltamethrin (Butox®) (one µl/ml)

deltamethrin revealed low larval mortality (l9.83, 11.1 and 10.1%, respectively).

Discussion

Synthetic chemical acaricides are the most popular method currently being used for tick control. Widespread use of deltamethrin has led to the emergence of deltamethrin resistance. Nanotechnology can help to solve many technical problems in several applications, such as in agriculture, development of antimicrobial, drug carriers, and insecticides formulations [32,33]. Layered double hydroxide (LDH) formulations have been used in drug delivery because of their easy synthesis, controllable size, biocompatibility, and they give the intercalated drug perfect coverage (as interact between two substance for synthesis of a good effective drug) [34]. Therefore, the ability of LDH nanomaterials has been demonstrated as a drug delivery system for ciprofloxacin to fight bacterial infection of the middle ear of rabbits [35]. Consequently, the adulticidal and larvicidal effects of deltamethrin-(Butox®) loaded nanocomposites of Zn-Fe LDH, Zn-Al-GA LDH, and Fe-NPs against *R. annulatus* ticks were evaluated through the adult immersion test (AIT) and the larval packet test (LPT), respectively.

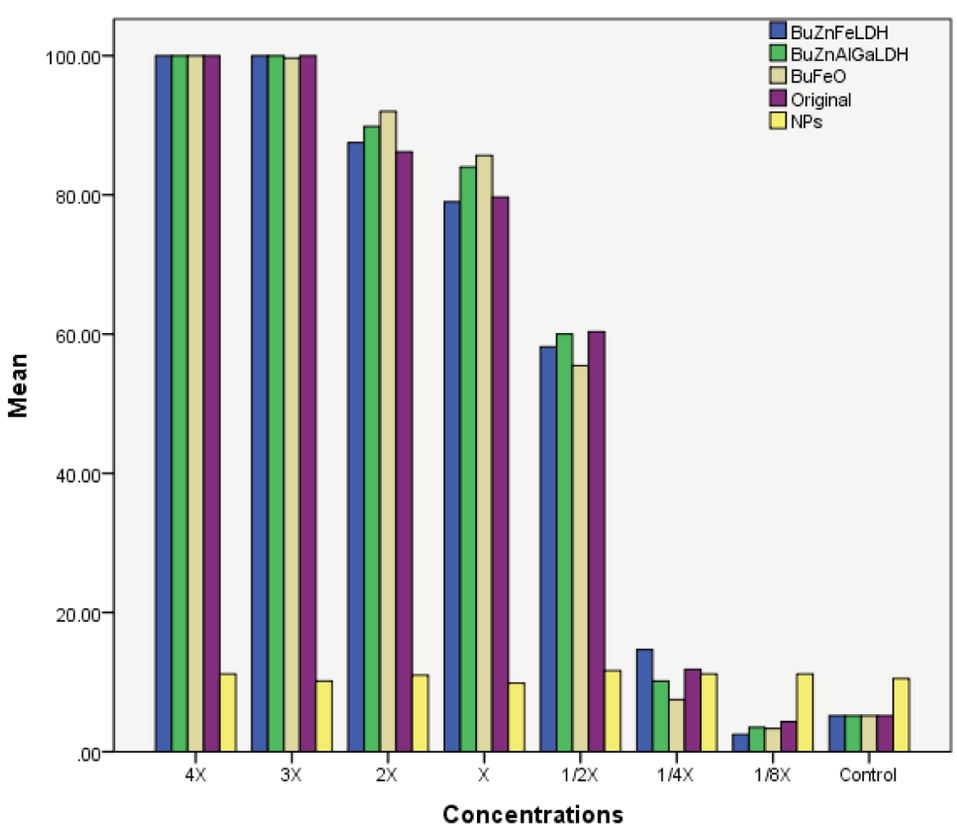

Figure 7. Larval mortality treated by deltamethrin and its loaded nanoforms at different concentrations

The used NCs (Zn-Fe LDH, Zn-Al-GA LDH, and Fe-NPs) were prepared and loaded with deltamethrin. Its interaction with deltamethrin (Butox®) was confirmed by XRD and FT-IR, which revealed successful loading. The prepared Zn-Fe LDH and Zn-Al-GA LDH resembled the typical XRD patterns of hydrotalcite-like LDH materials [36–38]. The FT-IR spectrum of Zn-Fe LDH is similar to that reported by [38,39].

No mortality was observed in the adult ticks treated with deltamethrin even at high concentrations. Deltamethrin resistance is prevalent among the tick isolates from the study area, as previously reported [5,8]. Consequently, the loaded forms of deltamethrin with Zn-Fe LDH, Zn-Al-GA LDH, and Fe-NPs at high concentrations (2X, 3X, and 4X) showed no mortality in adult ticks, but only a reduction in egg production and a decrease in the egg production index. A mutation in the sodium-channel of the *R. annulatus* tick (C190A in domain II) was identified as the major cause of the resistance [8]. Moreover, there is no significant difference ($P \geq 0.05$) between the effect of deltamethrin and its freshly loaded NCs against *R. annulatus* larvae at any concentration. The larval mortality of 100% was observed with treatment by deltamethrin and its freshly loaded forms at high concentrations (3X and 4X). Therefore, the used NCs had no effect on the efficacy of deltamethrin. Our results are comparable with the results of another study [40] that reported a reduction in egg production of *R. microplus* tick treated by cinnamon oil (nanocapsules or nanoemulsions). Also, no effects were recorded on *R. annulatus* treated with deltamethrin/Ag NPs [24]. Contrary to the results of the present study, the iron oxide nanoparticles (Fe-NPs) were lethal to *Hyalomma* spp. [41]. Moreover, deltamethrin/ZnO caused 100% mortality of adult *R. annulatus* tick and larvae [24]. Also, 93.33% mortality was reported in larvae and adults of *R. microplus* treated by deltamethrin loaded on Ag NPs and neem leaf extract [42]. Over all, the loading of deltamethrin on these NCs did not change its efficacy against the resistant isolates of *R. annulatus* ticks.

In this study, Zn-Fe LDH-, Zn-Al-GA LDH-, and Fe-O-NPs conjugated with deltamethrin caused low level of decrease in the egg production index of the treated resistant adult *R. annulatus* ticks. Therefore, the acaricidal activity of deltamethrin was not improved after loading it with these nanocomposites.

Acknowledgements

The authors appreciate veterinarians who helped during tick collection. We introduce great thank to Prof. Saeed El-Ashram for helping in the manuscript editing.

References

[1] Ducornez S., Barre N., Miller R.J., Garine-Wichatitsky M. 2005. Diagnosis of amitraz resistance in *Boophilus microplus* in New Caledonia with modified Larval Packet Test. *Veterinary Parasitology* 130(3–4): 285–292. doi:10.1016/j.vetpar.2005.04.018

[2] Ghosh S., Azhahianambi P., de la Fuente J. 2006. Control of ticks of ruminants with special emphasis on livestock farming system in India – present and future possibilities for integrated control: a review. *Experimental Applied Acarology* 40(1): 49–66. doi:10.1007/s10493-006-9022-5

[3] Martins R.M. 2006. Estudo in vitro da ação acaricida do óleo essencial da gramínea Citronela de Java (*Cymbopogon winterianus* Jowitt) no carrapato *Boophilus microplus* [*In vitro* study of the acaricidal activity of the essential oil from the Citronella of Java (*Cymbopogon winterianus* Jowitt) to the tick *Boophilus microplus*]. *Revista Brasileira de Plantas Medicinais* 8(2): 71–78 (in Portuguese with summary in English).

[4] de Campos-Pereira M., Bahia-Labruna M., Szabo M., Marcondes-Klafe G. 2008. *Rhipicephalus* (*Boophilus*) *microplus*: biologia, controle e resistencia. MetVet Livros, São Paulo (in Portuguese).

[5] Aboelhadid S.M., Arafa W.M., Mahrous L.N., Fahmy M.M., Kamel A.A. 2018. Molecular detection of *Rhipicephalus* (*Boophilus*) *annulatus* resistance against deltamethrin in middle Egypt. *Veterinary Parasitology: Regional Studies and Reports* 13: 198–204. doi:10.1016/j.vprsr.2018.06.008

[6] Patarroyo J.H., Vargas M.I., Gonzáles C.Z., Gusmán F., Martins-Filho O.A., Afonso L.C.C., Valente F.L., Peconick A.P., Marciano A.P., Patarroyo V.A.M., Sossai S. 2009. Immune response of bovines stimulated by synthetic vaccine SBm7462® against *Rhipicephalus* (*Boophilus*) *microplus*. *Veterinary Parasitology* 166(3–4): 333–339. doi:10.1016/j.vetpar.2009.09.036

[7] Cruz R., Guerrero F.D., Miller R.J., Vivas R.I., Tijerina M., Garcia D.I., Ortiz R., Cornel A.J., McAbee R.D., Diaz M.A. 2009. Molecular survey of pyrethroid resistance mechanism in Mexican field populations of *Rhipicephalus* (*Boophilius*) *microplus*. *Parasitology Research* 105: 1145–1153. doi:10.1007/s00436-009-1539-1

[8] Arafa W.M., Klafke G.M., Tidwell J.P., Perez de Leon A.A., Esteve-Gassent M. 2020. Detection of single

nucleotide polymorphism in the para-sodium channel gene of *Rhipicephalus annulatus* populations from Egypt resistant to deltamethrin. *Tick and Tick-borne Diseases* 11(5): article number 101488. doi:10.1016/j.ttbdis.2020.101488

[9] Bhanu S., Archana S., Ajay K., Bhatt J.L., Bajpai S.P., Singh P.S., Vandana B. 2011. Impact of deltamethrin on environment, use as an insecticide and its bacterial degradation-a preliminary study. *International Journal of Environmental Sciences* 1(5): 977–985. doi:10.6088/ijessi.0010520027

[10] Balcomb B., Singh M., Singh S. 2015. Synthesis and characterization of layered double hydroxides and their potential as nonviral gene delivery vehicles. *Chemistry Open* 4(2): 137–145. doi:10.1002/open.201402074

[11] Wang J., Hu J., Zhang S. 2010. Studies on the sorption of tetracycline onto clays and marine sediment from seawater. *Journal of Colloid and Interface Science* 349: 578–582. doi:10.1016/j.jcis.2010.04.081

[12] Rives V., del Arco M., Martín C. 2014. Intercalation of drugs in layered double hydroxides and their controlled release: a review. *Applied Clay Science* 88–89: 239–269. doi:10.1016/j.clay.2013.12.002

[13] Cunha V.R.R., Guilherme V.A., De Paula E., De Araujo D.R., Silva R.O., Medeiros J.V.R., Leite J.R.S.A., Petersen P.A.D., Foldvari M., Petrilli H.M., Constantino V.R.L. 2016. Delivery system for mefenamic acid based on the nanocarrier layered double hydroxide: physicochemical characterization and evaluation of anti-inflammatory and antinociceptive potential. *Material Science and Engineering C* 58: 629–638. doi:10.1016/j.msec.2015.08.037

[14] Bouaziz Z., Soussan L., Janot J., Jaber M., Ben Haj Amara A., Balme S. 2018. Dual role of layered double hydroxide nanocomposites on antibacterial activity and degradation of tetracycline and oxytetracyline. *Chemosphere* 206: 175–183. doi:10.1016/j.chemosphere.2018.05.003

[15] Tezuka S., Chitrakar R., Sonoda A., Ooi K., Tomida T. 2004. Studies on selective adsorbents for oxo-anions. Nitrate ion-exchange properties of layered double hydroxides with different metal atoms. *Green Chemistry* 6(2): 104–109. doi:10.1039/B314938M

[16] Allou N.B., Saikia P., Borah A., Goswamee R.L. 2017. Hybrid nanocomposites of layered double hydroxides: an update of their biological applications and future prospects. *Colloid and Polymer Science* 295: 725–747. doi:10.1007/s00396-017-4047-3

[17] Wang X., Zhu X., Meng X. 2017. Preparation of a Mg/Al/Fe layered supramolecular compound and application for removal of Cr(VI) from laboratory wastewater. RSC *Advances* 7(56): 34984–34993. doi:10.1039/C7RA04646D

[18] Yasaei M., Khakbiz M., Zamanian A., Ghasemi E. 2019. Synthesis and characterization of Zn/Al-LDH@SiO_2 nanohybrid: intercalation and release behaviour of vitamin C. *Material Science and Engineering C, Materials for Biological Applications* 103: article number 109816. doi:10.1016/j.msec.2019.109816

[19] Kang H.R., Da Costa Fernandes C.J., da Silva R.A., Constantino V.R.L., Koh I.H.J., Zambuzzi W.F. 2017. Mg-Al and Zn-Al layered hydroxides promote dynamic expression of marker genes in osteogenic differentiation by modulating mitogen-activated protein kinases. *Advanced Healthcare Materials* 7(4): article number 1700693. doi:10.1002/adhm.201700693

[20] Abo El-Ela F.I., Farghali A.A., Mahmoud R.K., Mohamed N.A., Abdel Moaty S.A. 2019. New approach in ulcer prevention and wound healing treatment using doxycycline and amoxicillin/LDH nanocomposites. *Scientific Reports* 9: article number 6418. doi:10.1038/s41598-019-42842-2

[21] Rodrigues G.R., Lopez-Abarrategui C., de la Serna Gomez I., Dias S.C., Otero-Gonzalez A.J., Franco O.L. 2019. Antimicrobial magnetic nanoparticles based-therapies for controlling infectious diseases. *International Journal of Pharmaceutics* 555: 356–367. doi:10.1016/j.ijpharm.2018.11.043

[22] Dadfar S.M., Roemhild K., Drude N.I., von Stillfried S., Knuchel R., Kiessling F., Lammers T. 2019. Iron oxide nanoparticles: diagnostic, therapeutic and theranostic applications. *Advanced Drug Delivery Reviews* 138: 302–325. doi:10.1016/j.addr.2019.01.005

[23] Gandhi P.R., Jayaseelan C., Mary R.R., Mathivanan D., Suseem S.R. 2017. Acaricidal, pediculicidal and larvicidal activity of synthesized ZnO nanoparticles using *Momordica charantia* leaf extract against blood feeding parasites. *Experimental Parasitology* 181: 47–56. doi:10.1016/j.exppara.2017.07.007

[24] Arafa W.M., Mohammed A.N., Abo El-Ela F.I. 2019. Acaricidal efficacy of deltamethrin-zinc oxide nanocomposite on *Rhipicephalus* (*Boophilus*) *annulatus* tick. *Veterinary Parasitology* 268: 36–45. doi:10.1016/j.vetpar.2019.03.002

[25] Alharbi N.S., Govindarajan M., Kadaikunnan S., Khaled J.M., Almanaa T.N., Alyahya S.A., Al-anbr M.N., Gopinath K., Sudha A. 2018. Nanosilver crystals capped with *Bauhinia acuminata* phytochemicals as new antimicrobials and mosquito larvicides. *Journal of Trace Elements in Medicine and Biology* 50: 146–153. doi:10.1016/j.jtemb.2018.06.016

[26] Mushinskiy A.A., Aminova E.V., Korotkova A.M. 2018. Evaluation of tolerance of tubers *Solanum tuberosum* to silica nanoparticles. *Environmental Science and Pollution Research* 25(34): 34559 –34569. doi:10.1007/s11356-018-3268-4

[27] Aboelhadid S.M., Mahran H.A., El-Ela F.A.I.,

Shokeir K.M., Henedy K.H., Gadelhaq S.M., Mahmoud A.A., Abdel-Baki A.S., Al-Quraishy S., Abdel-Tawab H. 2020. Synthesis of nanocomposites layered double hydroxide via *Ocimum basilicum* and its acaricidal efficacy against multi-resistance *Rhipicephalus annulatus* tick. *Journal of Biomed Nanotechnology* 16(12): 1765–1775. doi:10.1166/jbn.2020.3005

[28] Kameshima Y., Sasaki H., Isobe T., Nakajima A., Okada K. 2009. Synthesis of composites of sodium oleate/Mg-Al-ascorbic acid-layered double hydroxides for drug delivery applications. *International Journal of Pharmaceutics* 381(1): 34–39. doi:10.1016/j.ijpharm.2009.07.021

[29] Mohammed A.N., Radi A.M., Khaled R., Abo El-Ela F.I., Kotp A.A. 2020. Exploitation of new approach to control of environmental pathogenic bacteria causing bovine clinical mastitis using novel anti-biofilm nanocomposite. *Environmental Science and Pollution Research* 27(34): 42791-42805. doi:10.1007/s11356-020-10054-1

[30] Drummond R.O., Gladney W.J., Whetstone T.M., Ernst S.E. 1971. Laboratory testing of insecticides for control of the winter tick. *Journal of Economic Entomology* 64(3): 686–688. doi:10.1093/jee/64.3.686

[31] Pirali-Kheirabdi K., Haddadzadeh H., Razzaghi-Abyaneh M., Bokaie S., Zare R., Ghazavi M., Shams-Ghahfarokhi M. 2007. Biological control of *Rhipicephalus* (*Boophilus*) *annulatus* by different strains of *Metarhizium anisopliae*, *Beauveria bassiana* and *Lecanicillium psalliotae* fungi. *Parasitology Research* 100: 1297–1302. doi:10.1007/s00436-006-0410-x

[32] Ajitha B., Reddy Y.A.K., Jeon H.J., Ahn C.W. 2018. Synthesis of silver nanoparticles in an ecofriendly way using *Phyllanthus amarus* leaf extract: antimicrobial and catalytic activity. *Advanced Powder Technology* 29: 86–93. doi:10.1016/j.apt.2017.10.015

[33] Ravichandran V., Vasanthi S., Shalini S., Shah S.A.A., Harish R. 2016. Green synthesis of silver nanoparticles using *Atrocarpus altilis* leaf extract and the study of their antimicrobial and antioxidant activity. *Materials Letters* 180: 264–267. doi:10.1016/j.matlet.2016.05.172

[34] Xu Z.P., Lu G.Q. 2006. Layered double hydroxide nanomaterials as potential cellular drug delivery agents. *Pure and Applied Chemistry* 78(9): 1771–1779. doi:10.1351/pac200678091771

[35] Hesse D., Bader M., Bleich A., Smoczek A., Glage S., Kieke M., Behrens P., Muller P.P., Esser K., Stieve M., Prenzler N.K. 2013. Layered double hydroxides as efficient drug delivery system of ciprofloxacin in the middle ear: an animal study in rabbits. *Journal of Materials Science: Materials in Medicine* 24(1): 129–136. doi:10.1007/s10856-012-4769-1

[36] Younes H.A., Khaled R., Mahmoud H.M., Nassar H.F., Abdelrahman M.M., Abo El-Ela F.I., Taha M. 2019. Computational and experimental studies on the efficient removal of diclofenac from water using ZnFe-layered double hydroxide as an environmentally benign absorbent. *Journal of Taiwan Institute of Chemical Engineers* 102: 297–311. doi:10.1016/j.jtice.2019.06.018

[37] Zaher A., Taha M., Farghali A.A., Mahmoud R.K. 2020. Zn/Fe LDH as a clay-like adsorbent for the removal of oxytetracycline from water: combining experimental results and molecular simulations to understand the removal mechanism. *Environmental Science and Pollution Research* 27: 12256–12269. doi:10.1007/s11356-020-07750-3

[38] Moaty S.A., Farghali A., Khaled R. 2016. Preparation, characterization and antimicrobial applications of Zn-Fe LDH against MRSA. *Materials Science and Engineering* C 68: 184–193. doi:10.1016/j.msec.2016.05.110

[39] Yang Q., Wang S., Chen F., Luo K., Sun J., Gong C., Yao F., Wang X., Wu J., Li X. 2017. Enhanced visible-lightdriven photocatalytic removal of refractory pollutants by Zn/Fe mixed metal oxide derived from layered double hydroxide. *Catalysis Communications* 99: 15–19. doi:10.1016/j.catcom.2017.05.010

[40] dos Santos D.S., Boito J.P., Santos R.C.V., Quatrin P.M., Ourique A.F., dos Reis J.H., Debert R.R., Glombowsky P., Klauck V., Boligon A.A., Baldissera M.D., Da Silva A.S. 2017. Nanostructured cinnamon oil has the potential to control *Rhipicephalus microplus* ticks on cattle. *Experimental and Applied Acarology* 73(1): 129–138. doi:10.1007/s10493-017-0171-5

[41] Norouzi R., Kazemi F., Siyadatpanah A. 2020. Acaricidal effect of Iron nanoparticles against *Hyalomma* spp. *in vitro*. *Journal of Zoonotic Diseases* 4(3): 44–53. doi:10.22034/jzd.2020.10895

[42] Avinash B., Venu R., Alpha Raj M., Srinivasa Rao K., Sriatha C., Prasad T.N. 2017. In vitro evaluation of acaricidal activity of noval green silver nanoparticles against deltamethrin resistance *Rhipicephalus* (*Boophilus*) *microplus*. *Veterinary Parasitology* 237: 130–136. doi:10.1016/j.vetpar.2017.02.017

Received 11 August 2021
Accepted 28 October 2021